J. Fluid Mech. (2005), *vol.* 533, *pp.* 171–181.
doi:10.1017/S0022112005004246 Printed in the United Kingdom

Evolution of packets of surface gravity waves over smooth topography

By E. S. BENILOV, J. D. FLANAGAN AND C. P. HOWLIN

Department of Mathematics, University of Limerick, Ireland

(Received 14 April 2004 and in revised form 11 December 2004)

Weakly nonlinear packets of surface gravity waves over topography are governed by a nonlinear Schrödinger equation with variable coefficients. Using this equation and assuming that the horizontal scale of topography is much larger than the width of the packet, we show that, counter-intuitively, the amplitude of a shoaling packet decays, while its width grows. Such behaviour is a result of the fact that the coefficient of the nonlinear term in the topography-modified Schrödinger equation decreases with depth. Furthermore, there exists a critical depth, h_{cr}, where this coefficient changes sign – if the packet reaches h_{cr}, it disperses.

1. Introduction

The dynamics of surface gravity waves over bottom topography is one of the classical problems of fluid mechanics. It has been thoroughly studied in various formulations, including monochromatic waves (see Mei 1983) and shallow-water solitons (Grimshaw 1970; Ostrovsky & Pelinovsky 1970). However, an important particular case has been overlooked, as there seem to be virtually no results on shoaling of wave packets – which omission seems even stranger if one recalls the significance of this problem for oceanography. The only exception is the paper by Barnes & Peregrine (1995), who showed that the behaviour of a shoaling packet is quite different to that of a shoaling monochromatic wave. It turned out that the amplitude of the former is much lower than what the monochromatic theory predicts, as the packet tends to spread out – and this effect is more marked for slowly varying topography. However, no quantitative result was obtained which would link the parameters of the packet to the bottom topography over which it travels.

The present paper addresses the above omission. In § 2, we formulate the problem mathematically and, in § 3, examine it asymptotically, assuming that the depth variations are slow (i.e. the horizontal scale of topography is much larger than the width of the packet). In § 4, the asymptotic results will be compared to, and confirmed by, numerical simulations of the governing equation.

2. Formulation

Consider surface gravity waves in a basin with an uneven bottom (see figure 1). We shall assume that both topography and waves are one-dimensional, i.e. the depth h of the basin and the elevation η of the surface depend on a single horizontal variable, x (η also depends on the time t). We shall further assume that all our variables are non-dimensionalized using a characteristic depth h_0 and the acceleration due to

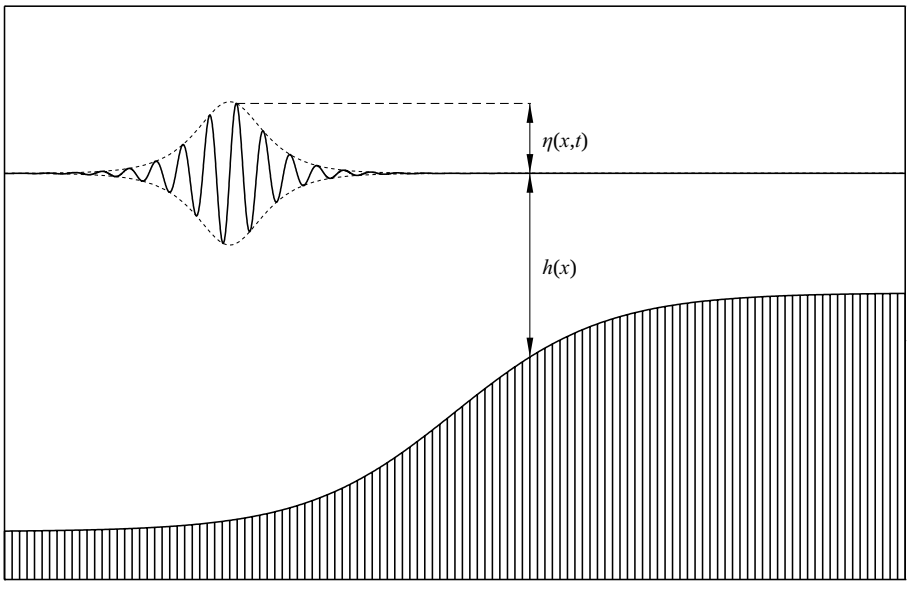

FIGURE 1. Formulation of the problem: a packet of surface gravity waves over topography.

gravity, g,

$$x = \frac{x_*}{h_0}, \qquad t = \frac{g^{1/2} t_*}{h_0^{1/2}}, \qquad \eta = \frac{\eta_*}{h_0}, \qquad h = \frac{h_*}{h_0},$$

where the asterisks mark the corresponding dimensional variables.

In this paper, we are concerned with weakly nonlinear quasi-monochromatic waves (packets), which can be characterized by a frequency ω. If the bottom were flat, ω would correspond to a certain value of the wavenumber k determined by the dispersion relation of surface gravity waves,

$$\omega^2 = k \tanh kh. \tag{2.1}$$

If h depends on x (uneven bottom), (2.1) can still be used as a means of finding k, which will, however, depend on x (i.e. the frequency of the wave is fixed, while its wavenumber changes as it propagates over topography – see Djordjevic & Redekopp (1978), or any textbook on waves in non-homogeneous media). To justify the use of (2.1) for an uneven bottom, $h(x)$ should be a slowly changing function of x, i.e. its spatial scale L_h should be much larger than the wavelength $2\pi k^{-1}$.

Under these assumptions, the packet is represented by

$$\eta(x,t) = \mathrm{Re}\left\{ A(x,t) \exp\left[\mathrm{i} \int k(x)\, \mathrm{d}x - \mathrm{i}\omega t \right] \right\},$$

where A is a slowly varying function (its spatial and time scales must exceed $2\pi k^{-1}$ and $2\pi\omega^{-1}$, respectively). $A(x,t)$ is governed by a nonlinear Schrödinger equation with varying coefficients (NSVC) – see Djordjevic & Redekopp (1978):

$$\mathrm{i}\left(\frac{\partial A}{\partial x} + \frac{1}{c_g} \frac{\partial A}{\partial t} + \mu A \right) - \alpha \frac{\partial^2 A}{\partial t^2} - \beta A |A|^2 = 0, \tag{2.2}$$

where

$$c_g(x) = \frac{1}{2\omega}(\tanh kh + kh\,\mathrm{sech}^2 kh) \tag{2.3}$$

is the group velocity of surface gravity waves, and

$$\alpha = \frac{1}{2\omega c_g}\left(\frac{2\omega h \tanh kh}{c_g} + 1 - \frac{h}{c_g^2}\right),$$
$$\beta = \frac{1}{2\omega^3 c_g}\left\{3k^4 + 2\omega^4 k^2 - \omega^8 - \frac{[2\omega k - c_g(\omega^4 - k^2)]^2}{h - c_g^2}\right\},$$
$$\mu = \frac{(1-\tanh^2 kh)(1 - kh\tanh kh)}{\tanh kh + kh(1-\tanh^2 kh)}\frac{\mathrm{d}(kh)}{\mathrm{d}x}. \tag{2.4}$$

Observe also that the NSVC equation (2.2) is written in the form where the spatial coordinate x is the 'evolutionary' variable (which role is usually played by t).

Before we proceed, it is instructive to consider the case of a flat bottom, where the coefficients of (2.2) become constant,

$$c_g = \text{const}, \qquad \mu = 0, \qquad \alpha = \text{const}, \qquad \beta = \text{const}.$$

Provided that

$$\alpha\beta > 0, \tag{2.5}$$

(2.2) admits a two-parameter family of exact solutions describing steadily propagating envelope solitons,

$$A = \sqrt{\frac{2\alpha}{\beta}}\lambda\,\mathrm{sech}\lambda\tau\,\exp\left(\frac{\mathrm{i}v\tau}{2\alpha} + \frac{4\mathrm{i}\lambda^2 x}{4+v^2}\right), \tag{2.6}$$

where

$$\tau = t - \left(\frac{1}{c_g} + v\right)x, \tag{2.7}$$

and λ and v are arbitrary parameters. In what follows, the expression

$$\max\{|A|^2\} = \frac{2\alpha\lambda^2}{\beta}$$

will be referred to as the amplitude of the wave packet, and λ^{-1} as its width. Finally, v characterizes the packet's translation speed (or, to be precise, v is proportional to the difference between the translation speed and c_g).

In the next section, we shall examine what happens to (2.6) in the case of variable depth.

3. Asymptotic analysis

When studying the evolution of envelope solitons using the NSVC equation (2.2), one needs to distinguish three asymptotic limits, involving the width λ^{-1} of the soliton and the spatial scale L_h of $h(x)$:

$$\lambda^{-1} \gg L_h, \tag{3.1}$$
$$\lambda^{-1} \sim L_h, \tag{3.2}$$
$$\lambda^{-1} \ll L_h. \tag{3.3}$$

Limit (3.1) has been examined by Djordjevic & Redekopp (1978), whereas (3.2) does not allow analytical treatment. Limit (3.3), in turn, has been studied for the case

of linear dependence of α and β on x, with attention mainly focused on the points where one of the two coefficients vanishes (e.g. Karpman & Maslov 1982; Malomed & Shrira 1991; Clarke *et al.* 1999). In the present paper, we shall consider the general case of α and β (as long as they satisfy (3.3)). Physically, this approximation can be applied to long ($2\pi k^{-1} \sim 50$–$500\,\mathrm{m}$) surface waves in the ocean, travelling over a slowly varying continental shelf.

In accordance with (3.3), we introduce a slow spatial variable,

$$X = \varepsilon x, \tag{3.4}$$

where $\varepsilon = \lambda^{-1}/L_h$ is a small parameter. Then, equation (2.2) becomes

$$\mathrm{i}\left(\varepsilon\frac{\partial A}{\partial X} + \frac{1}{c_g}\frac{\partial A}{\partial t} + \mu A\right) + \alpha\frac{\partial^2 A}{\partial t^2} + \beta A\,|A|^2 = 0. \tag{3.5}$$

We shall seek a solution in the form

$$A = B(X,\tau)\exp\left[\frac{\mathrm{i}v(X)\tau}{2\alpha} + \frac{\mathrm{i}}{\varepsilon}\int\frac{4\lambda^2(X)}{4+v^2(X)}\,\mathrm{d}X\right], \tag{3.6}$$

where

$$\tau = t - \frac{1}{\varepsilon}\int\left[\frac{1}{c_g(X)} + v(X)\right]\mathrm{d}X \tag{3.7}$$

((3.6)–(3.7) extend the envelope-soliton solution (2.6)–(2.7) to the case of variable depth). Substituting (3.6) into (3.5), we obtain

$$-\lambda^2 B + \alpha\frac{\partial^2 B}{\partial\tau^2} + \beta B|B|^2 = \varepsilon\left[\tau B\frac{\partial}{\partial X}\left(\frac{v}{2\alpha}\right) - \mathrm{i}\left(\frac{\partial B}{\partial X} + \mu B\right)\right]. \tag{3.8}$$

Seek a solution of (3.8) in the form of a series,

$$B = B^{(0)} + \varepsilon B^{(1)} + \cdots.$$

The first two orders of expansion yield

$$-\lambda^2 B^{(0)} + \alpha\frac{\partial^2 B^{(0)}}{\partial\tau^2} + \beta B^{(0)}\left|B^{(0)}\right|^2 = 0, \tag{3.9}$$

$$-\lambda^2 B^{(1)} + \alpha\frac{\partial^2 B^{(0)}}{\partial\tau^2} + \beta\left(2B^{(1)}\left|B^{(0)}\right|^2 + B^{(0)2}B^{(1)*}\right) = \tau B^{(0)}\frac{\partial}{\partial X}\left(\frac{v}{2\alpha}\right) - \mathrm{i}\left(\frac{\partial B^{(0)}}{\partial X} + \mu B^{(0)}\right). \tag{3.10}$$

Assume that $B(X,\tau)$ is bounded as $\tau \to \pm\infty$; in this case, the solution to (3.9) is

$$B^{(0)} = \sqrt{\frac{2\alpha}{\beta}}\lambda\,\mathrm{sech}\,\lambda\tau, \tag{3.11}$$

which corresponds to the usual envelope soliton. Next, we separate the real and imaginary parts of (3.10),

$$\lambda^2 B_r + \alpha\frac{\partial^2 B_r}{\partial\tau^2} + 3\beta B^{(0)2}B_r = \tau B^{(0)}\frac{\partial}{\partial X}\left(\frac{v}{2\alpha}\right), \tag{3.12}$$

$$\lambda^2 B_i + \alpha\frac{\partial^2 B_i}{\partial\tau^2} + \beta B^{(0)2}B_i = -\left(\frac{\partial B^{(0)}}{\partial X} + \mu B^{(0)}\right), \tag{3.13}$$

where $B_r = \mathrm{Re}B^{(1)}$ and $B_i = \mathrm{Im}B^{(1)}$. Equations (3.12) and (3.13) are linear non-homogeneous ODEs, and the operators on their left-hand sides are self-adjoint. As can be verified by inspection, the corresponding homogeneous ODEs have solutions bounded as $\tau \to \pm\infty$,

$$B_r = \frac{\partial B^{(0)}}{\partial \tau}, \qquad B_i = B^{(0)}.$$

Then, the full (non-homogeneous) ODEs (3.12) and (3.13) have bounded solutions only if their right-hand sides are orthogonal to the corresponding solutions of their homogeneous versions, i.e.

$$\int_{-\infty}^{\infty} \tau B^{(0)} \frac{\partial B^{(0)}}{\partial \tau}\, \mathrm{d}\tau \frac{\partial}{\partial X}\left(\frac{v}{2\alpha}\right) = 0, \tag{3.14}$$

$$\int_{-\infty}^{\infty} B^{(0)} \left(\frac{\partial B^{(0)}}{\partial X} + \mu B^{(0)}\right) \mathrm{d}\tau = 0. \tag{3.15}$$

Since

$$\int_{-\infty}^{\infty} \tau B^{(0)} \frac{\partial B^{(0)}}{\partial \tau}\, \mathrm{d}\tau = -\frac{1}{2} \int_{-\infty}^{\infty} B^{(0)2}\, \mathrm{d}\tau \neq 0,$$

it follows from (3.14) that

$$\frac{v}{2\alpha} = \mathrm{const}_1. \tag{3.16}$$

Next, (3.15) can be rearranged into

$$\frac{\partial}{\partial X} \int_{-\infty}^{\infty} B^{(0)2}\, \mathrm{d}\tau + 2\mu \int_{-\infty}^{\infty} B^{(0)2}\, \mathrm{d}\tau = 0$$

and integrated,

$$\int_{-\infty}^{\infty} B^{(0)2}\, \mathrm{d}\tau \exp\left[2 \int \mu(X)\, \mathrm{d}X\right] = \mathrm{const}_2.$$

Taking into account expression (3.11) for $B^{(0)}$ and expression (2) for μ, we obtain

$$\frac{4\alpha\lambda}{\beta}(\tanh kh + kh\, \mathrm{sech}^2 kh) = \mathrm{const}_2. \tag{3.17}$$

Observe that the expression in brackets is proportional to c_g – compare (3.17) and (2.3).

Equations (3.16) and (3.17) determine the dependence of v and λ (and, hence, the velocity and amplitude of the wave packet) on x. Interestingly, they can be also obtained through a simple, although non-rigorous, argument based on the conservation laws of the NSVC equation – see the Appendix.

Equations (3.16) and (3.17) are the main results of the present paper.

4. Examples, numerical simulations, and discussion

Let the depth of the basin be

$$h(x) = 1 - \Delta h \tanh[\gamma(x - x_0)], \tag{4.1}$$

which describes a depth variation of amplitude Δh and width γ^{-1}, located at $x = x_0$ (see figure 1). Then, before choosing a specific example, recall that our asymptotic results hold only if the topographic term in the NSVC equation is much smaller than

the other terms. Estimating these terms for topography (4.1) and solution (3.6), we obtain

$$\gamma \ll \lambda^2.$$

We should also keep in mind that the NSVC equations has been derived under the assumption that the length of the carrier wave is much smaller than the width of the packet, i.e.

$$\lambda \ll k.$$

Finally, we want the bottom at $x = 0$ to be essentially flat, i.e.

$$\gamma x_0 \gg 1.$$

To satisfy the above assumptions, we put

$$x_0 = 2000, \qquad \gamma = 0.002, \tag{4.2}$$

$$k = 2 \qquad \text{at} \qquad x = 0, \tag{4.3}$$

$$\lambda = 0.1 \qquad \text{at} \qquad x = 0. \tag{4.4}$$

To put (4.2)–(4.4) in an oceanographic context, assume that the characteristic depth is, say, $h_0 = 100\,\text{m}$. Then,

$$l \approx 300\,\text{m}, \qquad \Lambda = 1\,\text{km}, \qquad L = 50\,\text{km},$$

where $l = 2\pi h_0 k^{-1}$ is the (dimensional) length of the carrier wave, $\Lambda = h_0\lambda^{-1}$ is the length of the packet, and $L = h_0\gamma^{-1}$ is the characteristic scale of the depth change. The above parameters are consistent with a packet of oceanic swell propagating over a continental shelf.

First, we shall consider relatively small depth variation, say,

$$\Delta h = 0.2. \tag{4.5}$$

The evolution of λ was calculated using formula (3.17), and the resulting amplitude of the packet is plotted in figure 2. Observe that, unlike monochromatic waves (see Mei 1983) or shallow-water solitons (Grimshaw 1970; Ostrovsky & Pelinovsky 1970), the amplitude of the shoaling packet decreases. This tendency was observed in all examples considered.

In order to verify this counter-intuitive conclusion, the exact NSVC equation (2.2) has been simulated numerically with the initial condition

$$A = \sqrt{\frac{2\alpha}{\beta}}\lambda\,\text{sech}\lambda t \exp\left(\frac{\text{i}vt}{2\alpha}\right) \qquad \text{at} \qquad x = 0, \tag{4.6}$$

where λ is given by (4.4) and $v = 0.1$. The solution was assumed periodic in t, with a period that would be sufficiently large to eliminate interaction of two successive solitary waves. The condition of periodicity allowed us to use the pseudo-spectral method for the t-derivatives in equation (2.2), and we used the Runge–Kutta scheme for the x-derivative.

The results are shown in figure 2, which demonstrates that the agreement between the asymptotic and numerical solution is quite good.

We have also carried out simulations for larger values of γ, which correspond to a steeper depth variation. For $\gamma \lesssim 0.05$, the evolution of the wave packet was qualitatively the same, i.e. it would spread out while its amplitude decayed. For larger γ fission was observed, i.e. the main packet shed 'secondary' solitons. Note, however, that the amplitudes of those were always much smaller than that of the main packet.

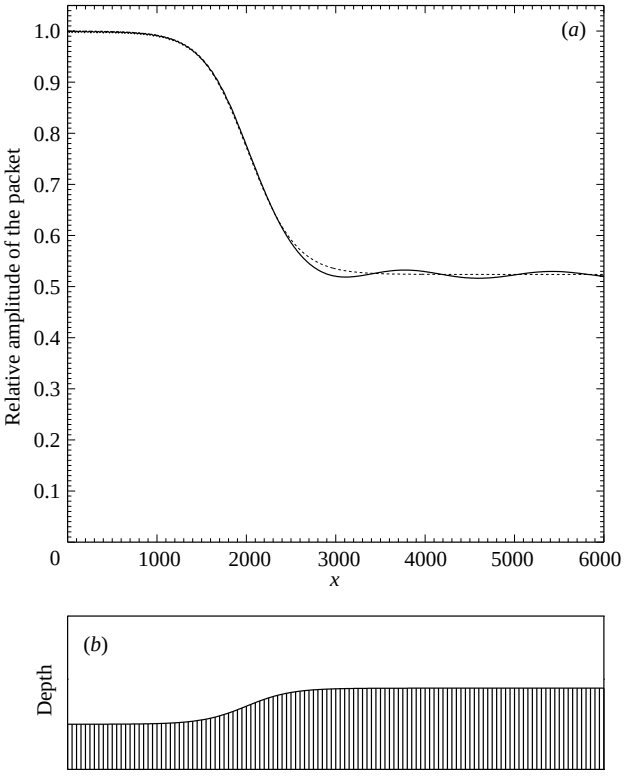

FIGURE 2. Shoaling of a wave packet with parameters (4.3)–(4.4) over topography (4.1)–(4.2), (4.5). (*a*) Relative amplitude of the packet (scaled by its initial value) *vs.* x. Solid line shows the numerical solution of the exact initial value problem (2.2), (4.6); dotted line shows the asymptotic solution (3.17). (*b*) The corresponding topography.

In order to illustrate what happens for a stronger depth variation, consider

$$\Delta h = 0.6, \tag{4.7}$$

with all other parameters being the same as before. In this case, the asymptotic formula (3.17) predicts that, at $x \approx 2400$, the packet's amplitude vanishes and its width becomes infinite – which essentially means that the packet disperses. This conclusion agrees reasonably well with a direct simulation of the NSVC equation (2.2) – see figure 3.

In order to understand why this occurs, use (3.17) to express the amplitude of the packet,

$$\frac{2\alpha\lambda^2}{\beta} = \frac{\text{const}_2^2}{8}\,\frac{\beta}{\alpha[\tanh kh + kh(1-\tanh^2 kh)]^2}. \tag{4.8}$$

Next, recall that

$$\alpha > 0 \qquad \text{for all } kh,$$

whereas

$$\begin{aligned} \beta &> 0 \qquad \text{if } kh \gtrsim 1.363, \\ \beta &= 0 \qquad \text{if } kh \approx 1.363, \\ \beta &< 0 \qquad \text{if } kh \lesssim 1.363 \end{aligned}$$

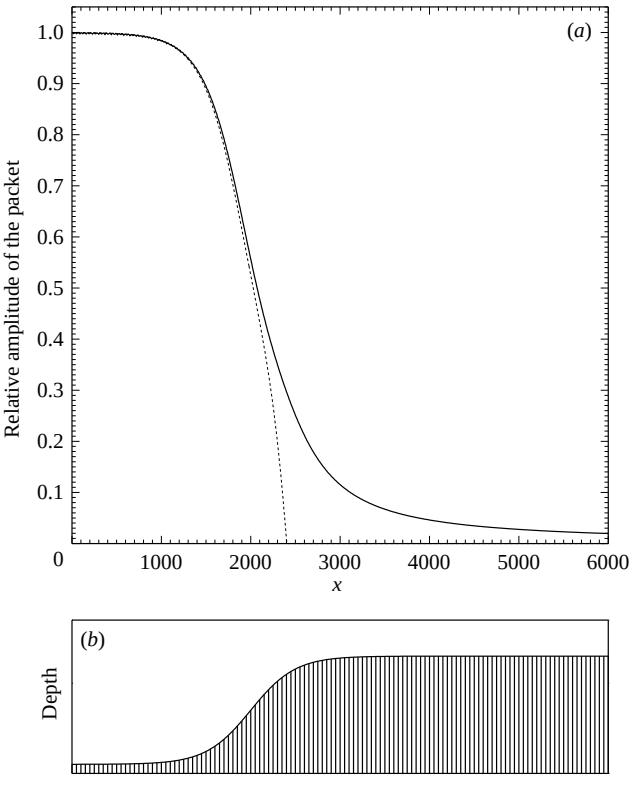

FIGURE 3. Shoaling of a wave packet with parameters (4.3)–(4.4) over topography (4.1)–(4.2), (4.7). (*a*) Relative amplitude of the packet (scaled by its initial value) *vs.* x. Solid line shows the numerical solution of the exact initial value problem (2.2), (4.6); dotted line shows the asymptotic solution (3.17). (*b*) The corresponding topography.

(the critical value of $kh \approx 1.363$ was originally calculated by Benjamin & Feir 1967). If $h(x)$ becomes sufficiently small, kh reaches the critical value, and the amplitude of the packet vanishes (see (4.8)). Beyond this point $\alpha\beta < 0$, and the packet may no longer exist as a coherent solitary wave.

It is illustrative to rewrite (4.8) in the form

$$\frac{\text{amplitude of the packet}}{\text{initial amplitude of the packet}} = \frac{\alpha(0)\beta(x)}{\alpha(x)\beta(0)} \left\{ \frac{\tanh k(0) + k(0)[1 - \tanh^2 k(0)]}{\tanh kh + kh(1 - \tanh^2 kh)} \right\}^2,$$

where it is assumed that the packet starts from $x = 0$ and $h(0) = 1$ (the latter condition implies that the problem was non-dimensionalized using the (dimensional) depth at $x = 0$. Then, we can show the dependence of the packet's (relative) amplitude on ω and h, where h is the depth at the packet's current location – see figure 4.

There is a simple criterion which allows one to distinguish the cases where the packet disperses from those where it does not. Recall that, at all x, the carrier wave satisfies the dispersion relation (2.1). Then, multiply (2.1) by $h\omega^{-2}$ and apply to the critical point (i.e. simply put $kh = 1.363$), which yields

$$h_{cr} \approx 1.195\omega^{-2}, \tag{4.9}$$

where h_{cr} is the depth at the critical point. This is, essentially, the desired criterion: if $h(x) > h_{cr}$, the packet passes over the depth variation as a coherent solitary wave and

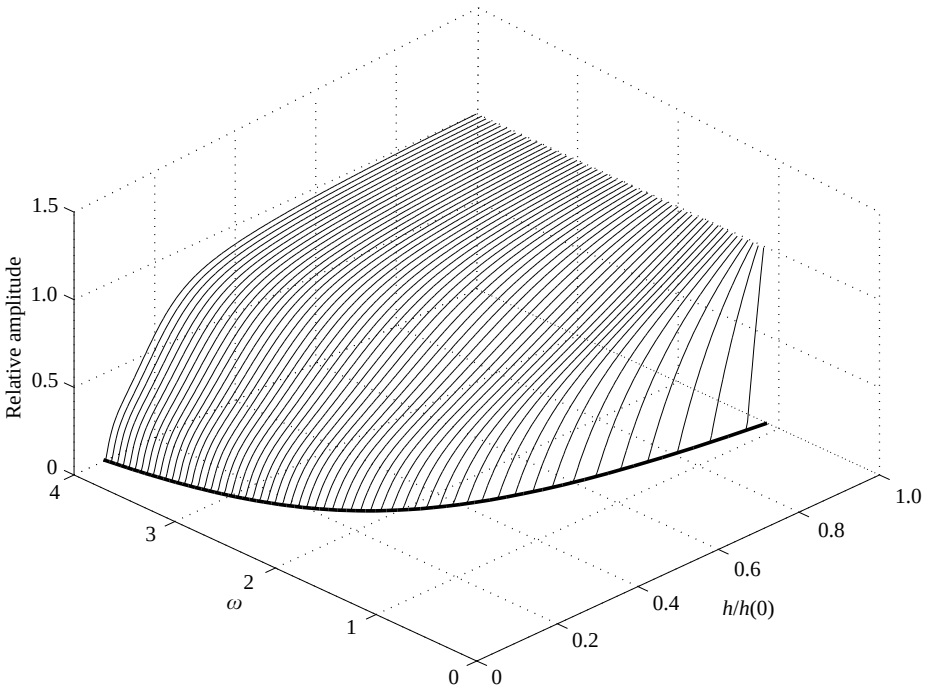

FIGURE 4. The amplitude of the packet, relative to its initial amplitude, *vs.* the non-dimensional frequency ω and relative depth $h(x)/h(0)$ (it is implied here that, initially, the packet is at $x=0$). Cross-sections corresponding to a fixed ω show the 'trajectories' of the wave packet as it travels over varying depth. The cut-off curve (bold line) shows the critical depth, where the packet's amplitude vanishes – see (4.9).

disperses otherwise. We shall also rewrite condition (4.9) in dimensional form,

$$h_{cr} \approx 1.195 g\omega^{-2}, \tag{4.10}$$

where g is the acceleration due to gravity and ω is the dimensional frequency of the carrier wave. Then, (4.10) can be illustrated as follows: let the packet come from 'deep water', where $kh \gg 1$ and $\omega \approx \sqrt{gk}$. For this case, (4.10) predicts that

$$h_{cr} \approx 0.190 l,$$

where l is the initial length of the carrier wave. Thus, for a shoaling packet coming from deep water with a wavelength of, say, 50 m, the critical depth is approximately 10 m.

Finally, we shall illustrate the importance of the nonlinear effects in the problem at hand. To do so, we replace the original NSVC equation (2.2) with its linear equivalent

$$\mathrm{i}\left(\frac{\partial A}{\partial x} + \frac{1}{c_g}\frac{\partial A}{\partial t} + \mu A\right) - \alpha\frac{\partial^2 A}{\partial t^2} = 0. \tag{4.11}$$

The initial-value problem (4.11), (4.6) has been solved for parameters (4.3)–(4.4), (4.1)–(4.2), (4.7) – see figure 5. One can see that, in the absence of nonlinearity, the packet almost immediately spreads out and disperses.

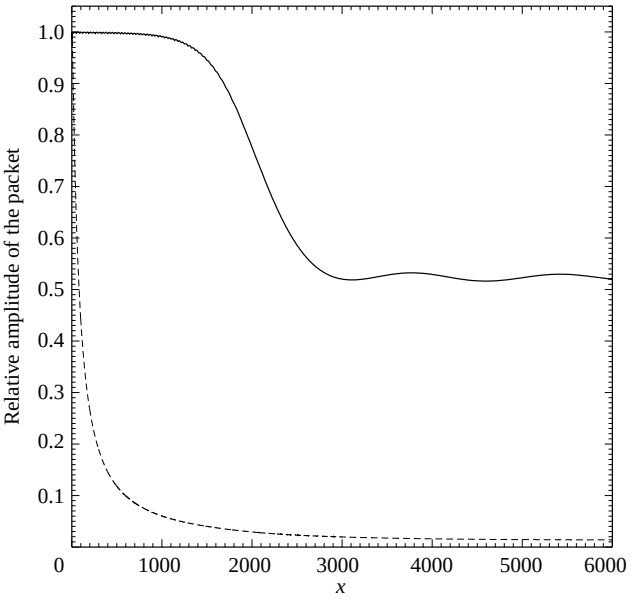

FIGURE 5. Shoaling of a wave packet with parameters (4.3)–(4.4) over topography (4.1)–(4.2), (4.7). Solid line shows the numerical solution of the full nonlinear initial value problem (2.2), (4.6); dashed line shows the corresponding linear solution (obtained through (4.11), (4.6)).

5. Concluding remarks

We have examined how a packet of surface gravity waves evolves over slowly varying topography. Assuming that the packet can be 'locally' described by an envelope soliton, we related its amplitude and velocity to the 'local' depth (see equations (3.16)–(3.17)). It turned out that, unlike monochromatic waves or shallow-water solitons, the amplitude of a shoaling packet decays. Moreover, if the depth reaches a certain critical value (determined by condition (4.10)), the coefficient of the nonlinear term in the nonlinear Schrödinger equation with variable coefficients changes sign, and the packet disperses.

Note that, strictly speaking, the asymptotic equations (3.16)–(3.17) are not applicable near the critical point. We shall not dwell on this question, but refer the reader to Malomed & Shrira (1991) and Clarke *et al.* (1999) where it is examined in detail. We also note that it would be interesting to compare the present results with simulations of the full surface-wave equations similar to those carried out by Barnes & Peregrine (1995) (the latter work does not quite cover the parameter regime considered here).

Appendix. Derivation of (3.16) and (3.17) from conservation laws

It turns out that the dynamics of a wave packet over slowly changing topography can be deduced from the conservation laws of the NSVC equation (2.2).

Assuming that A decays sufficiently fast as $t \to \pm\infty$, one can verify that (2.2) has two conservation laws,

$$\frac{\mathrm{d}}{\mathrm{d}x}\int_{-\infty}^{\infty}\left(A\frac{\partial A^*}{\partial t}-\frac{\partial A}{\partial t}A^*\right)\mathrm{d}t=0 \tag{A 1}$$

and

$$\frac{\mathrm{d}}{\mathrm{d}x}\left[(\tanh kh + kh\,\mathrm{sech}^2 kh)\int_{-\infty}^{\infty}|A|^2\,\mathrm{d}t\right]=0. \tag{A 2}$$

Physically, (A 1) and (A 2) reflect conservation of the net fluxes of momentum and wave action, passing through a fixed point x between $t=-\infty$ and $t=\infty$. The energy flux, to leading order, coincides with the action flux and, thus, does not result in a separate conservation law. Note also that (2.2) is a conservative system and, as such, has a Hamiltonian – which, however, explicitly depends on the evolutionary variable x and, hence, is not conserved.

Now, assume that the main contribution to the net momentum and wave action comes from the leading-order solution – which, in turn, can be calculated using (3.6), (3.11):

$$A\approx\sqrt{\frac{2\alpha}{\beta}}\lambda\,\mathrm{sech}\lambda\tau\,\exp\left[\frac{\mathrm{i}v(X)\tau}{2\alpha}+\frac{\mathrm{i}}{\gamma}\int\frac{4\lambda^2(X)}{4+v^2(X)}\,\mathrm{d}X\right], \tag{A 3}$$

with X, τ given by (3.4), (3.7). Substituting (A 3) into (A 1), (A 2) and carrying out the integration, we obtain (3.16), (3.17), respectively.

The above calculation can be viewed as a simple, heuristic alternative to the perturbation expansion presented in § 3.

REFERENCES

Barnes, T. & Peregrine, D. H. 1995 Wave groups approaching a beach: Full irrotational flow computations. In *Coastal Dynamics 195, Proc. Intl Conf. on Coastal Research in Terms of Large Scale Experiments, Gdansk, Poland* (ed. W. R. Dally), pp. 116–127.

Benjamin, T. B. & Feir, J. E. 1967 The disintegration of wave trains on deep water. Part 1. *J. Fluid Mech.* **27**, 417–430.

Clarke, S. R., Clutterbuck, J., Grimshaw, R. H. J. & Malomed, B. A. 1999 Passage of a wave pulse through a zero-dispersion point in the nonlinear Schrödinger equation. *Phys. Lett.* A **262**, 434–444.

Djordjevic, V. D. & Redekopp, L. G. 1978 On the development of packets of surface gravity waves moving over an uneven bottom. *Math. Phys. Z. Angew.* **29**, 950–962.

Grimshaw, R. 1970 The solitary wave in water of variable depth. *J. Fluid Mech.* **42**, 639–656.

Karpman, V. I. & Maslov, E. M. 1982 Soliton propagation in slowly varying media. *Phys. Fluids* **25**, 1686–1687.

Malomed, B. A. & Shrira, V. I. 1991 Soliton caustics. *Physica* D **53**, 1–12.

Mei, C. C. 1983 *The Applied Dynamics of Ocean Surface Waves*, Wiley.

Ostrovsky, L. A. & Pelinovsky, E. N. 1970 Wave transformation on the surface of fluid of variable depth. *Sov. Phys. Izv. Atmos. Ocean. Phys.* **6**, 552–555.